2024 European Control Conference (ECC)
June 25-28, 2024. Stockholm, Sweden

Scaled graphs for reset control system analysis

Sebastiaan van den Eijnden, Thomas Chaffey, Tom Oomen, Maurice Heemels

Abstract— **Scaled graphs allow for graphical analysis of nonlinear systems, but are generally difficult to compute. The aim of this paper is to develop a method for approximating the scaled graph of reset controllers. A key ingredient in our approach is the generalized Kalman-Yakubovich-Popov lemma to determine *input specific* input-output properties of a reset controller in the time domain. By combining the obtained time domain properties to cover the full input space, an over-approximation of the scaled graph is constructed. Using this approximation, we establish a feedback interconnection result and provide connections to classical input-output analysis frameworks. Several examples show the relevance of the results for the analysis and design of reset control systems.**

I. Introduction

This paper is concerned with the development of a framework for graphical analysis and design of reset control systems. The development of reset controllers has a long history starting with the introduction of the Clegg integrator in 1958 [1]. A reset controller is a linear time-invariant (LTI) system in which (part of) the states are reset to certain values whenever conditions on the inputs, outputs, and states are satisfied [2], [3]. It has long been observed that introducing resets in an LTI control loop can overcome fundamental performance limitations of LTI control systems [2], [4].

Reset controllers are often not so easily embraced by control engineers in industry. This is largely due to the lack of general analysis and design techniques for reset control systems that comply with graphical methods through Nyquist and Bode diagrams, which still largely dominate the industrial (motion) control design practice today. Some graphical methods based on frequency-domain techniques exist for reset control system analysis [5], [6], [7], but these methods are specific to the situation at hand and may lead to conservative results. All in all, a generic analysis and design framework is still missing.

In this paper, we aim towards the development of a generic framework for graphical analysis and design of reset control systems by making use of the *scaled graph*. Scaled graphs have been introduced in [8], [9] in convex optimization, and the theory has recently been extended in [10], [11], [12], [13] for (incremental) input-output analysis of feedback systems. In particular, these works establish a generalization of the classical Nyquist stability theorem for LTI systems, and provide an elegant means for graphically verifying stability margins for nonlinear systems. Given these possibilities, the scaled graph seems to be a promising tool for graphical analysis and design of reset control systems.

The scaled graph of a linear operator was characterized in [14], and the scaled graph of an LTI system is related to its Nyquist diagram via a convexification procedure under a nonlinear change of coordinates [10], [14]. Unfortunately, a practical problem remains in obtaining the scaled graph of a nonlinear system as this requires characterizing the input-output behaviour of the system for an infinite (uncountable) number of possible inputs. At best, we can estimate the scaled graph by 'sampling' it with a finite set of inputs [12], or by using general input-output properties such as $\mathcal{L}_2$-gain and/or passivity properties that are guaranteed to hold for all possible inputs. The approximation that results from both these approaches, however, may not accurately reflect the actual scaled graph; either we under-estimate it, thereby losing accuracy in the analysis, or we over-estimate it, possibly making it too conservative. Currently, this forms the main bottleneck for applying the scaled graph as a practical tool for system analysis and design.

In view of the difficulties in computing and using the scaled graphs of nonlinear systems in general, and reset controllers in particular, this paper presents two main contributions. In our first main contribution, we provide a computational tool for estimating the scaled graph of a reset controller. Key in our approach is the extension of the generalized Kalman-Yakubovich-Popov (KYP) lemma for LTI systems [19], [20], [21] towards the class of reset control systems. Essentially, the generalized KYP lemma allows for splitting up the space of input signals into smaller subspaces of input signals, each to which we can associate different input-output properties by solving sets of linear matrix inequalities (LMIs). The idea bears some resemblance to methods for determining 'mixed' properties of systems as in [22], [23], [24], [11], [25]. Exploiting the generalized KYP lemma in this context is new, and provides a different avenue and perspective for characterizing 'mixed' properties of nonlinear systems. For our second contribution, we use the scaled graph estimates of reset controllers in formulating an interconnection result that allows for graphical stability analysis of (closed-loop) reset control systems. We connect this result to integral quadratic constraints (IQCs) [26].

This paper is organized as follows. We begin by treating the concepts of reset controllers, the scaled graph and the generalized KYP in Section II. We present our first main contribution in Section III in the form of a computational tool for the scaled graph of a reset controller. Our second

The research leading to these results has received funding from the European Research Council under the Advanced ERC Grant Agreement PROACTHIS, no. 101055384.

Sebastiaan van den Eijnden, Tom Oomen, and Maurice Heemels are with the Department of Mechanical Engineering, Eindhoven University of Technology, 5600 MB Eindhoven, The Netherlands. Thomas Chaffey is with the Department of Engineering, University of Cambridge, Trumpington Street, Cambridge CB2 IPZ. E-mail: s.j.a.m.v.d.eijnden@tue.nl

contribution is presented in Section IV, where we formulate a theorem for graphical stability analysis of reset control systems. Proofs of the main results and further details may be found in the submitted journal version of this paper [27]. All results are supported by illustrative examples. The main conclusions are summarized in Section V.

II. Background and main idea

In this section, we review reset controllers, scaled graphs and the generalized KYP lemma for LTI systems, and sketch the main idea that we pursue in this paper.

A. Reset controllers

Throughout this paper we study reset controllers that can be modelled as hybrid dynamical systems of the form

$$\mathcal{R}: \begin{cases} \dot{x}_r(t) & = A_r x_r(t) + B_r u(t) \quad \text{if } (x_r(t), u(t)) \in \mathcal{F} \\ x_r(t^+) & = R x_r(t) \qquad\qquad\quad \text{if } (x_r(t), u(t)) \in \mathcal{J} \\ y(t) & = C_r x_r(t) + D_r u(t), \end{cases} \tag{1}$$

with states $x_r(t) \in \mathbb{R}^n$, input $u(t) \in \mathbb{R}$, and output $y(t) \in \mathbb{R}$ at time $t \in \mathbb{R}_{\geq 0} = [0, \infty)$, and where $x_r(t^+) = \lim_{s \downarrow t} x_r(s)$. The matrix R defines the reset map, and the sets $\mathcal{F}$ and $\mathcal{J}$ denote the flow and jump sets, which are considered here as

$$\mathcal{F} = \left\{ \xi \in \mathbb{R}^{n+1} \mid \xi^\top M \xi \geq 0 \right\}, \tag{2a}$$

$$\mathcal{J} = \left\{ \xi \in \mathbb{R}^{n+1} \mid \xi^\top M \xi \leq 0 \right\}, \tag{2b}$$

where $\xi = [x_r^\top, u^\top]^\top$ and $M = M^\top$. The class of reset controllers modeled as in (1), (2) encompasses well-known reset controllers from the literature, such as the (modified) Clegg integrator [1], [5], first-order reset elements (FORE) [2], [3] and second-order reset elements (SORE) [15].

We let $\mathcal{L}_2$ denote the space of square-integrable functions on the time axis $[0, \infty)$, with inner product and norm

$$\langle u, y \rangle := \int_0^\infty u(t) y(t) dt, \quad \text{and} \quad \|u\| = \sqrt{\langle u, u \rangle}.$$

We make the following standing assumption on the open-loop reset controller $\mathcal{R}$ in (1).

Assumption 1. *The open-loop reset controller $\mathcal{R}$ in* (1) *is $\mathcal{L}_2$-stable, in the sense that for initial conditions $x_r(0) = 0$, inputs u in $\mathcal{L}_2$ are mapped to states x_r, time derivatives $\dot{x}_r$ (excluding jumps), and outputs y all in $\mathcal{L}_2$, and there is no Zeno behaviour. We write then $y \in \mathcal{R}(u)$.*

B. Scaled graphs

We are primarily interested in characterizing the input-output behaviour of reset controllers in (1) through the notion of the scaled graph, aiming towards a graphical tool for reset control system design and analysis. For defining the scaled graph of a reset controller, we follow the ideas from [10], although we restrict our definition to a *non-incremental* form.

Definition 1. *The scaled graph of the reset controller $\mathcal{R}$ in* (1) *with initial condition $x_r(0) = 0$ is defined as*

$$\mathcal{SG}(\mathcal{R}) := \bigcup_{u \in \mathcal{L}_2} z(u), \tag{3}$$

where the set of complex numbers $z(u)$ is given by

$$z(u) := \left\{ \frac{\|y\|}{\|u\|} e^{\pm j \angle(u,y)} \mid u \neq 0, y \in \mathcal{R}(u) \right\} \tag{4}$$

with

$$\angle(u, y) := \arccos\left(\frac{\langle u, y \rangle}{\|u\| \|y\|} \right) \in [0, \pi], \tag{5}$$

and $z(0) = \{0\}$.

It is shown in [10] that, when $\mathcal{R}$ is linear and time-invariant, its scaled graph contains its Nyquist diagram. Scaled graphs of passive systems lie in the left-half plane, and the maximum modulus of the scaled graph gives an $\mathcal{L}_2$-gain bound for the system.

Estimating the scaled graph via the mentioned $\mathcal{L}_2$-gain and/or passivity approaches could be restrictive, as we can already see for LTI systems. For instance, when exciting a second-order LTI mass-spring-damper system with a sufficiently low-frequency sinusoidal input, the system behaves as a passive system as the output lag is less than 90 degrees. On the other hand, when exciting the system with a high-frequency sinusoidal input, passivity is violated but the amplitude of the output is small. Hence, these systems are not passive, nor do they possess a small $\mathcal{L}_2$-gain bound for every possible input. This example suggests that, instead of looking for input-output properties that hold for *all* possible inputs, it may be useful to consider input-output properties for the system that only hold true for *specific inputs* (see also the work on 'mixed' passive/small-gain systems in, e.g., [22], [23]). In this way, we may be able to find estimates for the scaled graph that better reflect the true input-output nature of the nonlinear system. In general, it is not immediately clear how to characterize input-specific input-output properties for generic systems, but for the class of LTI systems this can be done through application of the generalized KYP lemma [19], [20], which we discuss next.

C. Generalized KYP lemma

Consider an LTI system of the form

$$\dot{x}(t) = Ax(t) + Bu(t), \quad x(0) = 0, \tag{6}$$

with $x(t) \in \mathbb{R}^n$ the state, and $u(t) \in \mathbb{R}$ the input, for $t \in \mathbb{R}_{\geq 0}$. The generalized KYP lemma establishes equivalences between a set of LMIs and input-output properties of the system (6) expressed in time domain that only hold true for *specific inputs* that excite the system in a specific manner.

Theorem 1 ([20, Theorem 3])**.** *Consider the LTI system* (6) *and let a Hermitian matrix Θ, and a real parameter λ, be given. Assume that A is Hurwitz and* (6) *is controllable. Then, the following statements are equivalent:*

1) *There exist Hermitian matrices P and Q that satisfy the LMIs $Q \succeq 0$ and*

$$\begin{bmatrix} A & B \\ I & 0 \end{bmatrix}^* \begin{bmatrix} -Q & P \\ P & \lambda^2 Q \end{bmatrix} \begin{bmatrix} A & B \\ I & 0 \end{bmatrix} + \Theta \preceq 0. \tag{7}$$

2) *The time-domain inequality*

$$\int_0^\infty \begin{bmatrix} x(t) \\ u(t) \end{bmatrix}^* \Theta \begin{bmatrix} x(t) \\ u(t) \end{bmatrix} dt \leq 0 \tag{8}$$

holds for all solutions of (6) *with* $u \in \mathcal{L}_2$ *such that*

$$\int_0^\infty \dot{x}(t)^\top Q \dot{x}(t) dt \leq \lambda^2 \int_0^\infty x(t)^\top Q x(t) dt. \tag{9}$$

The result in Theorem 1 provides a computational tool for assessing *input-specific* properties of the LTI system in (6). The specific inputs are characterized through the inequality in (9). This inequality plays an important role as it essentially allows for splitting up the set of all input signals into two sets. That is, given a matrix Q and a number λ, simply stated there is a set of inputs that satisfy (9) with $Q \succeq 0$ (or in other words with '$\leq$') and there is a set of inputs that satisfy (9) with $-Q \succeq 0$ (or in other words with '$\geq$'). The union of these sets covers the full input space. Setting $Q = 0$ recovers the classical KYP lemma since then (9) holds for all inputs.

The role of the parameter λ in (9) can be better understood by re-writing (9) in the frequency-domain using Parseval's equality, that is

$$\int_0^\lambda (\omega^2 - \lambda^2) \hat{x}^* Q \hat{x} d\omega \leq \int_\lambda^\infty (\lambda^2 - \omega^2) \hat{x}^* Q \hat{x} d\omega,$$

where $\hat{x}$ is the Fourier transform of x. The inequality roughly states that the content of $\hat{x}$ in the range $|\omega| \leq \lambda$ is smaller than that in the remaining frequency range. The value of λ essentially characterizes how much certain frequency content (modes) of the system are excited by the corresponding inputs that satisfy (9).

The main idea pursued in this paper is to generalize the LMI conditions in Theorem 1 posed for LTI systems towards reset control systems, to provide a computational tool for verifying certain *input-specific* input-output properties in time-domain. In turn, combining these input-specific properties to cover the full input space (i.e., by considering both Q and $-Q$) then allows for bounding the scaled graph of a reset controller through a non-convex set.

III. Main result: Scaled graph computations

In this section we will formalize the idea described in the previous section and present our first main result in the form of a numerically tractable method for computing an overapproximation of the scaled graph of the reset controller.

A. Input-specific time-domain properties

The following theorem provides sufficient conditions for computing input-specific time-domain properties of reset controllers, and is the crucial step in our procedure for constructing the scaled graph.

Theorem 2. *Consider the open-loop reset controller* (1), (2) *and let Hermitian matrices* Θ *and* $Q \succeq 0$*, and a real parameter* λ *be given. Assume that* A_r *in* (1) *is Hurwitz and* $x_r(0) = 0$*. Suppose there exist real numbers* $\tau \neq 0$ *and* $\sigma \geq 0$ *and a Hermitian matrix* P *that satisfy the LMIs*

$$\begin{bmatrix} A_r & B_r \\ I & 0 \end{bmatrix}^* \begin{bmatrix} -\tau Q & P \\ P & \tau\lambda^2 Q \end{bmatrix} \begin{bmatrix} A_r & B_r \\ I & 0 \end{bmatrix} + \Theta + \sigma M \preceq 0, \tag{10}$$

$$R^\top P R - P \preceq 0, \tag{11}$$

where the matrices R *and* M *are given in* (1) *and* (2)*, respectively. Then, the time-domain inequality*

$$\int_0^\infty \begin{bmatrix} x_r(t) \\ u(t) \end{bmatrix}^* \Theta \begin{bmatrix} x_r(t) \\ u(t) \end{bmatrix} dt \leq 0 \tag{12}$$

holds for all solutions of (1)*,* (2) *with* $u \in \mathcal{L}_2$ *such that*

$$\tau \int_0^\infty \dot{x}_r(t)^\top Q \dot{x}_r(t) dt \leq \tau\lambda^2 \int_0^\infty x_r(t)^\top Q x_r(t) dt. \tag{13}$$

Note that τ in Theorem 2 can take positive or negative values, and essentially splits up the input space as the sign of τ determines whether $-\tau Q$ is positive or negative definite (see also the discussion after Lemma 1). Moreover, τ provides an additional decision variable in the LMIs.

For assessing input-specific input-output properties of the reset system in (1), we select Θ in (10) to be of the form

$$\Theta = \begin{bmatrix} C_r & D_r \\ 0 & I \end{bmatrix}^* \Pi \begin{bmatrix} C_r & D_r \\ 0 & I \end{bmatrix}, \text{ with } \Pi = \begin{bmatrix} a & b \\ b & c \end{bmatrix} \tag{14}$$

where $a, b, c \in \mathbb{R}$ can be chosen to represent properties such as passivity $(a, b, c) = (0, -1, 0)$ and finite-gain $(a, b) = (1, 0)$, $c < 0$ [16], [17]. We assume that $a \geq 0$ and $\det(\Pi) = ac - b^2 < 0$ for reasons that become clear in the next section.

B. Connections to the scaled graph

The matrix Π in (14) directly relates to the scaled graph in Definition 1. To see how, note that we may write

$$\begin{aligned} \int_0^\infty \begin{bmatrix} x \\ u \end{bmatrix}^* \Theta \begin{bmatrix} x \\ u \end{bmatrix} dt &= \int_0^\infty \begin{bmatrix} y \\ u \end{bmatrix}^\top \Pi \begin{bmatrix} y \\ u \end{bmatrix} dt \\ &= a\|y\|^2 + 2b\langle u, y \rangle + c\|u\|^2. \end{aligned} \tag{15}$$

Recalling the definition of the complex number $z(u)$ in (4), we find that $\mathrm{Re}\{z(u)\} = \langle u, y \rangle / \|u\|^2$. Then, assuming $u \neq 0$ and dividing (15) by $\|u\|^2$, (15) can be rewritten as $a|z|^2 + 2b\mathrm{Re}\{z\} + c$. When (15) is non-positive, i.e., (12) holds, this inequality defines a region in the complex plane given by

$$\mathcal{S}(\Pi) = \left\{ z \in \mathbb{C} \;\middle|\; \begin{bmatrix} z \\ 1 \end{bmatrix}^* \Pi \begin{bmatrix} z \\ 1 \end{bmatrix} \leq 0 \right\}. \tag{16}$$

Assuming $a \geq 0$ and $\det(\Pi) = ac - b^2 < 0$, the region described in (16) is convex and represents the inside of a (shifted) circle centred on the real axis, or a half plane.

The region $\mathcal{S}(\Pi)$ in (16) corresponds to a single input-output property characterized by Π, that holds for inputs satisfying (13). It is possible that for these inputs, other properties, characterized by different choices for Π may hold as well. For example, a system could behave passive for some signals and at the same time admit a small-gain for

other signals. Given $\lambda \in \mathbb{R}$ and $Q \succeq 0$, we define the set of matrices Π that verify the LMIs (10), (11) with $\tau > 0$ by

$$\mathbf{\Pi}_+(\lambda, Q) := \left\{ \Pi \in \mathbb{S}^{2\times 2} \mid (10), (11) \text{ feasible} \right\}. \quad (17)$$

In a similar way we can define the set $\Pi_-(\lambda, Q)$ when the LMIs are satisfied with $\tau < 0$. Through these sets, we can find a convex region in the complex plane that, given λ, and Q characterizes the input-output properties for those inputs satisfying (13). In particular, this region is given by

$$\boldsymbol{\mathcal{S}}_+(\lambda, Q) = \bigcap_{\Pi_+ \in \mathbf{\Pi}(\lambda, Q)} \mathcal{S}(\Pi). \quad (18)$$

We define $\boldsymbol{\mathcal{S}}_-(\lambda, Q)$ in a similar manner. Equipped with the sets in (18) that we can find by application of Theorem 2, we can find an over-approximation of the scaled graph of the reset system $\mathcal{R}$ in (1) as formalized in the next main result.

Theorem 3. *Given $\lambda \in \mathbb{R}$ and $Q \succeq 0$. The scaled graph of the reset system $\mathcal{R}$ in* (1) *satisfies*

$$\mathcal{SG}(\mathcal{R}) \subseteq \boldsymbol{\mathcal{S}}_-(, \lambda, Q) \cup \boldsymbol{\mathcal{S}}_+(\lambda, Q), \quad (19)$$

where $\boldsymbol{\mathcal{S}}_\pm(\lambda, Q)$ is defined in (18)*.*

Proof. We need to show that $\boldsymbol{\mathcal{S}}_-(\lambda, Q) \cup \boldsymbol{\mathcal{S}}_+(\lambda, Q)$ covers the full input space. This is immediate from (13) as any input satisfies (13) for either $\tau > 0$ or $\tau < 0$. □

It is important to note that for estimating different regions of the scaled graph we use a common matrix Q (up to some scaling with τ) to guarantee that (13) covers the full input space. Using a common matrix Q, however, may not be necessary and could introduce conservatism. Relaxing this constraint is considered for future work.

We conclude this section with an example demonstrating applicability of the computational tools for estimating the scaled graph of a reset controller.

Example 1. Consider a second-order reset element modelled as in (1) with system matrices given by

$$\left[\begin{array}{c|c} A_r & B_r \\ \hline C_r & D_r \end{array}\right] = \left[\begin{array}{cc|c} -1 & 0 & 1 \\ 1 & -1 & 0 \\ \hline 0 & 1 & 0 \end{array}\right], \quad (20)$$

and with the reset map and resetting condition given by

$$R = \begin{bmatrix} 0 & 0 \\ 0 & 0 \end{bmatrix}, \text{ and } M = \left[\begin{array}{c|c} M_{11} & 0 \\ \hline 0 & 0 \end{array}\right] = \left[\begin{array}{cc|c} 0 & 1 & 0 \\ 1 & 0 & 0 \\ \hline 0 & 0 & 0 \end{array}\right]. \quad (21)$$

This element represents the series interconnection of two first-order low-pass filters for which the states are reset to zero on the basis of the condition $x^\top M_{11} x \geq 0$. A Nyquist plot of the base linear system, i.e., the system without resets, is shown in Fig. 1.

We will assess passivity and small-gain properties of this reset element by considering matrices Π of the form

$$\Pi_{\text{passivity}} = \begin{bmatrix} 0 & -1 \\ -1 & 0 \end{bmatrix}, \text{ and } \Pi_{\text{gain}} = \begin{bmatrix} 1 & 0 \\ 0 & -\gamma^2 \end{bmatrix}. \quad (22)$$

First, we want to test whether these properties hold for *all* inputs u. Recall that this is guaranteed by feasibility of the LMIs in (7)–(11) for $Q = 0$. It turns out that for $\Pi_{\text{passivity}}$ no feasible solution exists, and thus the system does not satisfy the sufficient conditions (7)–(11) for passivity. For Π_{gain} a feasible solution was found with $\gamma = 1$. On the basis of this result, we conclude that the scaled graph is contained within the unit circle, indicated by the dashed black circle in Fig. 1.

Next, we test whether the passivity and small-gain properties hold for *specific* inputs. For this purpose, we solve the LMIs in Theorem 2 with a common value for $\lambda = 0.9868$ and $Q = \left[\begin{smallmatrix} 0.250 & 0.267 \\ 0.267 & 0.992 \end{smallmatrix}\right]$. It turns out that for $\tau = 1 > 0$ and $\tau = 10^{-7} > 0$ the LMIs are feasible for resepctively $\Pi_{\text{passivity}}$ and Π_{gain} with $\gamma = 1$, indicating that the reset system is passive with finite gain for all inputs satisfying (13) with $\tau > 0$. No feasible solution is found with $\Pi_{\text{passivity}}$ for $\tau < 0$, but we do find a solution for Π_{gain} with $\gamma = 0.51$ and with $\tau = -0.5 < 0$. Hence, for inputs satisfying (13) with $\tau < 0$, the system is not passive, but does possess a small-gain property. This result is not surprising given the characteristics of the base linear system, which possesses the same mixed passivity/small-gain property. Finally, we conclude that the scaled graph of the reset system is contained within the non-convex region $\{z \in \mathbb{C} \mid |z| \leq 0.51\} \cup \{z \in \mathbb{C} \mid |z| \leq 1 \text{ and } \mathrm{Re}\{z\} \geq 0\}$, which is illustrated in Fig. 1 in light grey. Note that this region is significantly smaller than the region obtained with only the small-gain result, i.e., the dashed black circle in Fig. 1.

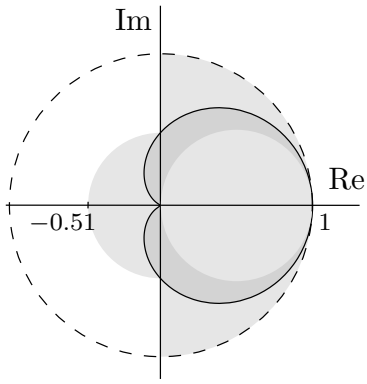

Fig. 1: Input-output characterizations of the reset controller. The scaled graph of the reset controller is bounded by the light grey region. The Nyquist plot of the base linear system is shown in black, and its scaled graph in dark grey.

IV. Main result: Feedback stability analysis

In this section, we present our second main contribution in the form of a theorem for assessing stability of the closed-loop system depicted in Fig. 2, where G represents a (possibly nonlinear) plant, and $\mathcal{R}$ is a reset element (1).

In the remainder of this section, stability is understood in the sense of $\mathcal{L}_2$-stability [17], [18], i.e., for zero initial states, inputs u in $\mathcal{L}_2$ are mapped to outputs y in $\mathcal{L}_2$. The feedback interconnection of Fig. 2 is said to be *well-posed* if the map $u \mapsto e$ is uniquely defined on all of $\mathcal{L}_2$ and is

causal. We define inversion in the complex plane via the transformation $re^{j\phi} \to (1/r)e^{j\phi}$, and the distance between two sets $A, B \subseteq \mathbb{C}$ by $\text{dist}(A, B) = \inf_{a\in A, b\in B} |a - b|$.

A. A general stability result

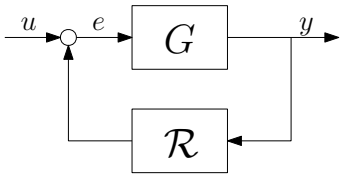

Fig. 2: Interconnection of a plant G and a reset element $\mathcal{R}$.

Theorem 4. *Consider the negative feedback interconnection depicted in Fig. 2 and suppose that G and $\mathcal{R}$ are $\mathcal{L}_2$-stable, as guaranteed by Assumption 1. Suppose that, for all $\mu \in (0, 1]$, the feedback interconnection of G and $\mu\mathcal{R}$ is well-posed. Moreover, suppose that for some λ the set $\bar{\boldsymbol{\mathcal{S}}}_\lambda := \boldsymbol{\mathcal{S}}_-(\lambda, Q) \cup \boldsymbol{\mathcal{S}}_+(\lambda, Q) \subseteq \mathbb{C}$ is non-empty. If there exists $r > 0$ such that, for all $\mu \in (0, 1]$,*

$$\text{dist}(\bar{\boldsymbol{\mathcal{S}}}_\lambda^{-1}, -\mu\mathcal{SG}(G)) \geq r, \tag{23}$$

then the feedback interconnection is $\mathcal{L}_2$-stable with an $\mathcal{L}_2$ gain bound of $1/r$.

Condition (23) in Theorem 4 essentially states that the scaled graph of G does not intersect with the region in the complex plane defined by $-\bar{\boldsymbol{\mathcal{S}}}_\lambda^{-1}$. This condition allows for a graphical test, as we demonstrate in the next example.

Example 2. Consider the interconnection in Fig. 2, where G is a stable LTI system described by the transfer function

$$G(s) = \frac{14s + 8}{s^5 + 13s^4 + 58s^3 + 96s^2 + 34s + 4.2} \tag{24}$$

and the reset controller is defined earlier in Example 1, that is, $\mathcal{R}$ is modelled as in (1) with system matrices given by (20) and (21). To test stability of the feedback interconnection we plot both $-\bar{\boldsymbol{\mathcal{S}}}_\lambda^{-1}$ (which corresponds to the inverse of the grey region in Fig. 1) and the scaled graph of G in (24) in the complex plane. The result is shown in Fig. 3 and demonstrates that condition (23) is satisfied, hence the closed-loop system is stable. Note that there is a gap between the scaled graphs, indicating a robustness margin and finite $\mathcal{L}_2$-gain of the closed loop.

Stability could not be verified solely on the basis of the scaled graph resulting from the small-gain property (which would require $\|G(j\omega)\| < 1$ for stability) nor on the basis of the passivity property, as neither $\mathcal{R}$ nor G are passive. Hence, by using a scaled graph approximation based on input specific input-output properties, we are able to relax the classical small-gain/passivity conditions.

B. Connections to IQCs

Scaled graphs are intimately related to the framework of IQCs. The final contribution in this paper, Theorem 5 below, establishes an initial connection between Theorem 4, and

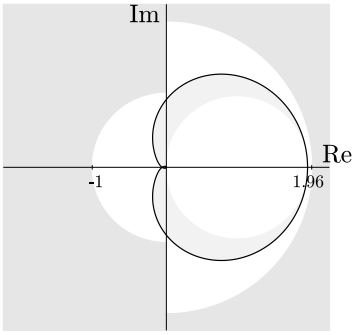

Fig. 3: Graphical test for verifying condition (23) in Theorem 4. The region $-\bar{\boldsymbol{\mathcal{S}}}_\lambda^{-1}$ is indicated in dark grey. The scaled graph of G in (24) is indicated in light gray. Note that this region is bounded by the Nyquist curve of G, shown in black.

IQCs for LTI systems whose scaled graphs lie within their Nyquist diagrams. We begin by characterizing this property.

Definition 2. *Let $G(s)$ be the transfer function of a stable LTI system. We say that $G(s)$ has a* Nyquist-bounded scaled graph *if, for all $0 \leq \theta \leq \pi$,*

$$\underset{\substack{z\in\overline{\mathcal{SG}}(G),\\ \arg z=\theta}}{\arg\max} |z| \in \{G(j\omega)\}_{\omega\in\mathbb{R}}. \tag{25}$$

Sufficient conditions for an LTI transfer function to have a Nyquist-bounded scaled graph are given in [27] in terms of conditions on the curvatures of the Nyquist diagram.

Theorem 5. *Consider the feedback interconnection shown in Fig. 2 where G is stable and LTI. Suppose that G has a Nyquist-bounded scaled graph and that for some λ and $Q \succeq 0$ the sets $\boldsymbol{\Pi}_\pm(\lambda, Q)$ in (17) are non-empty. Let the set $-\bar{\boldsymbol{\mathcal{S}}}_\lambda^{-1}$ be contained in the set $\{z \in \mathbb{C} \mid f(z) \geq 0\}$, with $f : \mathbb{C} \to \mathbb{R}$ a (non-smooth) function. If the inequality*

$$f(G(j\omega)) < 0 \tag{26}$$

is satisfied for all $\omega \in \mathbb{R} \cup \{\infty\}$, then the feedback interconnection of G and $\mathcal{R}$ is $\mathcal{L}_2$-stable.

To better understand how the result in Theorem 5, specifically condition (26), relates to input specific IQCs, we first consider an illustrative example.

Example 3. Consider again the interconnection in Fig. 2 with G given in (24) and $\mathcal{R}$ is given by (1) with (20), (21). Recall that for this reset controller we found mixed passivity/small-gain properties characterized through the matrices in (22). For this example, it can be seen from Fig. 3 that the region $-\bar{\boldsymbol{\mathcal{S}}}_\lambda^{-1}$ is contained in $\{z \in \mathbb{C} \mid f(z) \geq 0\}$, where f is given by

$$f(z) = \begin{cases} z^2 - 1.96 & \text{for all } \angle z \in (-\pi/2, \pi/2), \\ z^2 - 1 & \text{for all } \angle z \notin [-\pi/2, \pi/2]. \end{cases} \tag{27}$$

Since the scaled graph of G is bounded by its Nyquist curve (see Fig. 3), condition (26) in Theorem 5 can be formulated

in an IQC-like manner, that is

$$|G(j\omega)| < 1.96 \text{ for all } \omega \in \Omega_1, \tag{28a}$$

$$|G(j\omega)| < 1 \text{ for all } \omega \in \Omega_2, \tag{28b}$$

where $\Omega_1 = \{\omega \in \mathbb{R} \cup \{\infty\} \mid \mathrm{Re}\{G(j\omega)\} \geq 0\}$ and $\Omega_2 = \{\omega \in \mathbb{R} \cup \{\infty\} \mid \mathrm{Re}\{G(j\omega)\} \leq 0\}$. Here we indeed recognize the input-dependent nature of the constraints. The frequency region Ω_1 relates to those inputs that excite the LTI system G in a manner such that it behaves as a passive system, and the constraint in (28a) accounts for situations where $\mathcal{R}$ is not passive. Similarly, the region Ω_2 relates to inputs that excite the LTI system G in a manner that it violates passivity but still admits small-gain behaviour, and condition (28b) accounts for large-gain behaviour of the reset controller $\mathcal{R}$. In comparison, the classical small-gain IQC requires $\|G(j\omega)\| < 1$ for all $\omega \in \mathbb{R} \cup \{\infty\}$, which is clearly violated as can be seen from the Nyquist curve of G in Fig. 3.

As demonstrated in the previous example, in cases where $\boldsymbol{\mathcal{S}}_{\pm}(\lambda, Q)$ consist of the finite intersection of circles and half-planes, the function $f(z)$ can, in fact, be written as a piecewise quadratic function of z. Then, condition (26) can be recast as a set of quadratic constraints on $G(j\omega)$ each of which only need to hold for some frequency range, instead of for all frequencies. This reflects the input-dependent nature of the integral time-domain inequalities in (12) that are used for constructing the scaled graph of reset controllers.

V. Conclusions

We present a computational tool for estimating the scaled graph of reset controllers. Key in our approach is the use of the generalized KYP lemma to estimate *input-specific* input-output properties of the reset controller in the time domain. Each property maps to a region in the complex plane that partly covers the scaled graph of the reset controller. By combining all properties, we obtain a possibly non-convex over-approximation of the scaled graph that is used in an interconnection result and supports graphical robust stability analysis of reset control systems.

In this paper, we have restricted our attention to the class of single-input single-output reset controllers, but we expect that the ideas apply to a much broader class of nonlinear systems, including multivariable systems, unstable systems and systems with time delay. Extending the results, tightening the estimates of the scaled graphs, for instance by allowing the matrix Π in (14) to be complex valued, and incremental analysis will be topics for future research.

Acknowledgements

The authors acknowledge Andrey Kharitenko for bringing some technicalities in Theorem 4 to their attention, and Rodolphe Sepulchre and Fulvio Forni for fruitful discussions.

References

[1] J.C. Clegg, 'A nonlinear integrator for servomechanisms,' *Transactions of the American Institute of Electrical Engineers, Part II: Applications and Industry*, 77(1), pp. 41-42, 1958.

[2] O. Beker, C.V. Hollot, and Y. Chait, 'Plant with integrator: An example of reset control overcoming limitations of linear feedback,' *IEEE Transactions on Automatic Control*, 46(11), pp. 1797-1799, 2001.

[3] D. Nešić, A.R. Teel, and L. Zaccarian, 'Stability and performance of SISO control systems with first order reset elements,' *IEEE Transactions on Automatic Control*, 56, pp. 2567-2582, 2011.

[4] G. Zhao, D. Nešić, Y. Tan, and C. Hua, 'Overcoming overshoot performance limitations of linear systems with reset control,' *Automatica*, 101, pp. 27-35, 2019.

[5] S.J.L.M. van Loon, K.G.J. Gruntjens, M.F. Heertjes, N. van de Wouw, and W.P.M.H. Heemels, 'Frequency-domain tools for stability analysis of reset control systems', *Automatica*, 82, pp. 101-108, 2017.

[6] A. Dastjerdi, A. Astolfi, S. HosseinNia, 'Frequency-domain stability methods for reset control systems', *Automatica*, 148, pp.110737, 2023.

[7] O. Beker, C.V. Hollot, Y. Chait, and H. Han, 'Fundamental properties of reset control systems,' *Automatica*, vol. 40, pp. 905-915, 2004.

[8] X. Huang, E. K. Ryu, and W. Yin, 'Tight coefficients of averaged operators via scaled relative graph,' Journal of Mathematical Analysis and Applications, vol. 490, no. 1, 2020.

[9] E.K. Ryu, R. Hannah, and W. Yin, 'Scaled relative graphs: nonexpansive operators via 2D Euclidean geometry,' *Mathematical Programming*, vol. 194, pp. 569–619, 2022.

[10] T. Chaffey, F. Forni and R. Sepulchre, 'Graphical Nonlinear System Analysis,' in *IEEE Trans. on Aut. Cont.*, 68(10), pp. 6067-6081, 2023.

[11] T. Chaffey, 'A rolled-off passivity theorem,' *Syst. & Cont. Lett.*, 162, 2022.

[12] T. Chaffey, F. Forni and R. Sepulchre, 'Scaled relative graphs for system analysis,' *60th IEEE Conference on Decision and Control*, Austin, TX, USA, pp. 3166-3172, 2021.

[13] T. Chaffey, A. Padoan, 'Circuit model reduction with scaled relative graphs,' *61st IEEE Conference on Decision and Control*, Cancun, Mexico, pp. 6530-6535, 2022.

[14] R. Pates, 'The scaled relative graph of a linear operator,' arXiv:2106.05650, 2021.

[15] L. Hazeleger, M. Heertjes and H. Nijmeijer, 'Second-order reset elements for stage control design,' in Proceedings of the American Control Conference (ACC), Boston, MA, USA, 2016, pp. 2643-2648.

[16] G. Zames, 'On the input-output stability of time-varying nonlinear feedback systems Part one: Conditions derived using concepts of loop gain, conicity, and positivity,' in *IEEE Transactions on Automatic Control*, vol. 11, no. 2, pp. 228-238, 1966.

[17] C.A. Desoer, and M. Vidyasagar, *Feedback systems: input-output properties*, Society for Industrial and Applied Mathematics, 2009.

[18] H.K. Khalil, *Nonlinear Systems (3rd ed.)*, Prentice Hall, Upper Saddle River, New Jersey, 2002.

[19] T. Iwasaki and S. Hara, 'Generalized KYP lemma: unified frequency domain inequalities with design applications,' in *IEEE Transactions on Automatic Control*, vol. 50, no. 1, pp. 41-59, 2005.

[20] T. Iwasaki, S. Hara, and A. L. Fradkov, 'Time domain interpretations of frequency domain inequalities on (semi)finite ranges,' *Systems & Control Letters*, vol. 54, no. 7, pp. 681-691, 2005.

[21] G. Pipeleers and L. Vandenberghe, 'Generalized KYP Lemma With Real Data,' in *IEEE Trans. on Aut. Con.*, vol. 56. pp. 2942-2946, 2011.

[22] W. M. Griggs, B.D.O. Anderson, and A. Lanzon, 'A "mixed" small gain and passivity theorem in the frequency domain,' *Systems & Control Letters*, vol. 56, no. 9–10, pp. 596-602, 2007.

[23] W. M. Griggs, B.D.O. Anderson, A. Lanzon, and M.C. Rotkowitz, 'Interconnections of nonlinear systems with "mixed" small gain and passivity properties and associated input–output stability results,', *Systems & Control Letters*, vol. 58, no. 4, pp. 289-295, 2009.

[24] J. R. Forbes and C. J. Damaren, "Synthesis of Optimal Finite-Frequency Controllers Able to Accommodate Passivity Violations,' *IEEE Trans. on Cont. Syst. Tech.*, vol. 21, no. 5, pp. 1808-1819, 2013.

[25] S. Patra and A. Lanzon, 'Stability Analysis of Interconnected Systems With "Mixed" Negative-Imaginary and Small-Gain Properties,' in *IEEE Trans on Aut. Cont.*, vol. 56, no. 6, pp. 1395-1400, 2011.

[26] A. Megretski and A. Rantzer, 'System analysis via integral quadratic constraints,' in *IEEE Trans. on Aut. Cont.*, 42(6), pp. 819-830, 1997.

[27] S.J.A.M. van den Eijnden, T. Chaffey, T. Oomen, and W.P.M.H. Heemels, 'Scaled graphs for reset control system analysis', ArXiv.

[28] A. Rantzer, 'On the Kalman—Yakubovich—Popov lemma', *Systems & Control Letters*, 28(1), pp.7–10, 1996.

[29] R.A. Freeman, 'On the Role of Well-Posedness in Homotopy Methods for the Stability Analysis of Nonlinear Feedback Systems', In Lecture Notes in Control and Information Sciences, pp. 43-82, 2022.